

Superconductivity and magnetism in the $\text{Sc}_{5-x}\text{Dy}_x\text{Ir}_4\text{Si}_{10}$ system

S. Ramakrishnan and K. Ghosh

Tata Institute of Fundamental Research, Bombay, India 400 005

Aravind D. Chinchure

Dr. Babasaheb Ambedkar Marathwada University, Aurangabad, India 431 004

Kristian Jonason,* V. R. Marathe, and Girish Chandra

Tata Institute of Fundamental Research, Bombay, India 400 005

(Received 24 June 1994; revised manuscript received 17 August 1994)

We have recently shown a possible coexistence of superconductivity and magnetism in the $\text{Sc}_{5-x}\text{Dy}_x\text{Ir}_4\text{Si}_{10}$ system from susceptibility (χ) and resistivity (ρ) measurements. In this paper, we present heat-capacity (C_p) data for the same system which establishes the bulk nature of antiferromagnetic ordering in $\text{Dy}_5\text{Ir}_4\text{Si}_{10}$ and the coexistence of bulk superconductivity and magnetism in $\text{Sc}_{3.5}\text{Ir}_{1.5}\text{Si}_{10}$. Our heat-capacity data on Dy samples show considerable contribution from the Schottky effect due to the crystal fields and we have proposed a model which fits well to the χ and C_p data of all the Dy samples with the same crystal field parameters.

I. INTRODUCTION

Most of the studies made on the coexistence of superconductivity and magnetism are mainly from RMO_6S_8 chalcogenides and RRh_4B_4 borides (R =rare earth).¹ In these systems superconductivity arises due to the Mo clusters and Rh clusters, respectively, while magnetism due to the rare-earth element. A previous study² has indicated that there is a possibility to observe coexistence of magnetism and superconductivity in the $\text{Sc}_{5-x}\text{Dy}_x\text{Ir}_4\text{Si}_{10}$ system at low temperatures. Recently, we have observed that coexistence of superconductivity and magnetism is possible in the ternary rare-earth silicides $\text{Sc}_{5-x}\text{Dy}_x\text{Ir}_4\text{Si}_{10}$ for $x=3.25$ and $x=3.5$,³ and in the ternary rare-earth germanides $\text{Y}_2\text{Dy}_3\text{Os}_4\text{Ge}_{10}$.⁴ The crystal structure of these compounds ($\text{Sc}_5\text{Co}_4\text{Si}_{10}$ type, $P4/mbm$) has no transition metal clusters responsible for the superconductivity and no direct transition-transition metal contact. This is in contrast to that of chalcogenides and borides which have been studied in great detail. We have also shown the presence of superzone effects in $\text{Dy}_5\text{Ir}_4\text{Si}_{10}$ at low temperatures.⁵ In this work, we report heat-capacity measurements on $\text{Sc}_{5-x}\text{Dy}_x\text{Ir}_4\text{Si}_{10}$ ($x=0, 1.5, \text{ and } 5$) from 1.6 to 35 K. We also present dc susceptibility data for the above samples from 1.5 to 300 K.

II. EXPERIMENTAL DETAILS

The samples were made by melting individual constituents (taken in stoichiometric proportions) in an arc furnace under a high-purity argon atmosphere. The purity of Si was 99.999% whereas the purity of Ir and the rare-earth elements (Sc and Dy) was 99.9% each. The alloys were remelted five to six times to ensure proper mixing. The x-ray powder diffraction pattern of the samples showed a tetragonal structure of the type $P4/mbm$ reported in earlier studies.^{2,6} The heat capacity in zero

field, between 1.6 and 35 K, was measured using an automated adiabatic calorimeter in which a calibrated germanium resistance thermometer (LAKE SHORE Inc., USA) was used as the temperature sensor in this range. The temperature dependence of the susceptibility (χ) was measured using a superconducting quantum interference device (Quantum Design, USA) in a field of 4 kOe from 5 to 300 K and a home built ac susceptometer⁷ in the temperature range from 1.5 to 30 K.

III. RESULTS AND DISCUSSION

A. Results

The temperature dependence of the heat capacity (C_p) of $\text{Sc}_5\text{Ir}_4\text{Si}_{10}$ is shown in Fig. 1 and the inset shows the same plot at low temperatures. The C_p jump at 8.4 K shows bulk superconducting ordering in this sample below this temperature. In the case of the $\text{Sc}_5\text{Ir}_4\text{Si}_{10}$ sample, C_p is fitted to the expression

$$C_p = \gamma T + \beta T^3 + \delta T^5, \quad (1)$$

where γ is due to the electronic contribution, β is due to the lattice contribution, and δ is due to anharmonicity in the lattice. The presence of a significant anharmonic contribution to the heat capacity in these silicides has already been reported by earlier studies.^{8,9} However, the values of γ , β , and δ from our measurement differ from those of an earlier study in $\text{Sc}_5\text{Ir}_4\text{Si}_{10}$.⁹ The value of the ratio $\Delta C/\gamma T_c$ is 1.8, which shows that the sample is an intermediate coupling superconductor.

The heat-capacity data fitted using Eq. (1) in the temperature range from 10 to 30 K yielded a γ value of 17.7 mJ/mol K², a β value of 1.18 mJ/mol K³, and a δ value of 1.13×10^{-4} mJ/mol K⁶. The γ value has been obtained by matching the entropy of the normal and superconducting state at T_c as suggested by Stewart, Meisner, and Ku.¹⁰ From the β value of 1.18 mJ/mol K⁴, we estimate

Θ_D to be 315 K using the relation

$$\Theta_D = \left[\frac{12\pi^4 N r k_B}{5\beta} \right]^{1/3}, \quad (2)$$

where N is the Avogadro's number, r is the number of atoms per formula unit, and k_B is the Boltzmann's constant. Using the value of Θ_D and T_c , we can estimate the electron-phonon scattering parameter λ from the McMillan theory¹¹ where λ is given by

$$\lambda = \frac{1.04 + \mu^* \ln(\Theta_D / 1.45 T_c)}{(1 - 0.62 \mu^*) \ln(\Theta_D / 1.45 T_c) - 1.04}. \quad (3)$$

Assuming $\mu^* = 0.1$, we find the value of λ to be 0.7, which puts $\text{Sc}_5\text{Ir}_4\text{Si}_{10}$ as an intermediate coupling superconductor. On the basis of purely thermodynamical arguments, the thermodynamic critical field at $T = 0$ K [$H_c(0)$] can be determined by integrating the entropy difference between the superconducting and normal states. From our experimental heat-capacity data, we obtain a value of 650 Oe for $H_c(0)$. One can also calculate the thermodynamical critical field $H_c(0)$ from the expression

$$[H_c(0)]^2 = \frac{\gamma T_c^2}{0.17}, \quad (4)$$

where γ is the heat capacity coefficient ($\text{erg}/\text{cm}^3 \text{K}^2$). This gives a value of $H_c(0)$ as 642 Oe. Our previous study¹² shows that the extrapolated experimental value of the upper critical field [$H_{c2}(0)$] at 0 K is 0.82 T. From this value of $H_{c2}(0)$, we can estimate the Ginzburg-Landau coherence length $\xi_{\text{GL}}(0)$ at $T = 0$ K from the relation

$$[\xi_{\text{GL}}(0)]^2 = \frac{\phi_0}{2\pi H_{c2}(0)}, \quad (5)$$

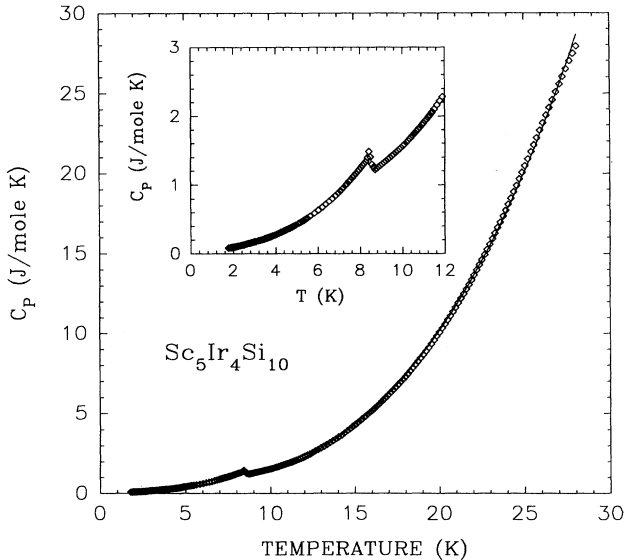


FIG. 1. The temperature dependence of the heat capacity of $\text{Sc}_5\text{Ir}_4\text{Si}_{10}$ from 1.7 to 30 K. The inset shows the same plot at low temperatures. The solid line in the main figure is a fit to Eq. (1) (see the text).

where $\phi_0 = 2.07 \times 10^{-7} \text{ G cm}^2$. This equation yields a value of 200 Å for $\xi_{\text{GL}}(0)$. Using the expression $H_{c2} = H_c 2^{1/2} \kappa$ (where $\kappa = \lambda_{\text{GL}} / \xi_{\text{GL}}$), we get the κ value as 8.9. From the value of $\xi_{\text{GL}}(0) = 200$ Å (determined earlier), we get a value of 1780 Å for the Ginzburg-Landau penetration depth $\lambda_{\text{GL}}(0)$. The value of the lower critical field at $T = 0$ K can be estimated using the relation¹³

$$H_{c1}(0) = \frac{H_c(0) \ln(\kappa)}{2^{1/2} \kappa}, \quad (6)$$

which yields a value of 113 Oe for the lower critical field at 0 K. This value of $H_{c1}(0)$ has to be verified with magnetization measurements on the same sample. Detailed magnetization measurements on this sample are in progress and will be reported elsewhere. The enhanced density of states can be calculated using $N^*(E_F) = 0.2121 \gamma / N$ where N is the number of atoms per formula unit and γ is expressed in $\text{mJ}/\text{mol K}^2$. The value of $N^*(E_F)$ is 0.2 states/(eV atom spin-direction) and the value of the bare density of states $N(E_F) = N^*(E_F) / (1 + \lambda) = 0.01$ states/(eV atom spin-direction). The normal-state and superconducting-state properties of $\text{Sc}_5\text{Ir}_4\text{Si}_{10}$ are given in Table I.

The heat capacity of $\text{Dy}_5\text{Ir}_4\text{Si}_{10}$ measured between 2 and 35 K, is shown in Fig. 2. A plot of C_p versus T^3 (not shown) showed a linear relationship in the temperature range of 15–35 K, which clearly indicates that the lattice contribution to C_p has βT^3 behavior with $\beta = 1.00 \text{ mJ}/\text{mol K}^4$. The magnetic heat capacity, obtained by subtracting the lattice contribution (βT^3) from the observed heat capacity and the corresponding values of entropy are shown in Fig. 3. The total entropy below T_N is $0.45R$ and is close to the value of $0.5R$ which is expected from a magnetic system whose crystal-field ground state is a doublet. A λ -type anomaly due to antiferromagnetic ordering is observed at 5.0 K. Above 8 K, a Schottky-type anomaly appears with a maximum at 32 K. Exactly the same behavior of the Schottky anomaly was observed by subtracting the heat capacity of the isomorphous non-magnetic compound $\text{Y}_5\text{Ir}_4\text{Si}_{10}$ from the observed heat capacity of $\text{Dy}_5\text{Ir}_4\text{Si}_{10}$. The temperature dependence of the heat capacity of $\text{Sc}_{3.5}\text{Dy}_{1.5}\text{Ir}_4\text{Si}_{10}$ is shown in Fig. 4.

TABLE I. Superconducting and normal-state properties of $\text{Sc}_5\text{Ir}_4\text{Si}_{10}$.

Parameter	Units	Value
T_c	K	8.5
γ	$\text{mJ}/\text{mol K}^2$	17.7
β	$\text{mJ}/\text{mol K}^4$	1.18
δ	$\text{mJ}/\text{mol K}^6$	1.13×10^{-4}
Θ_D	K	315
λ		0.7
$N^*(E_F)$	states/(eV atom spin)	0.2
$N(E_F)$	states/(eV atom spin)	0.01
ξ_{GL}	Å	200
λ_{GL}	Å	1780
$H_{c2}(0)$	Tesla	0.82
$H_{c1}(0)$	Tesla	0.0113
$H_c(0)$	Tesla	0.065

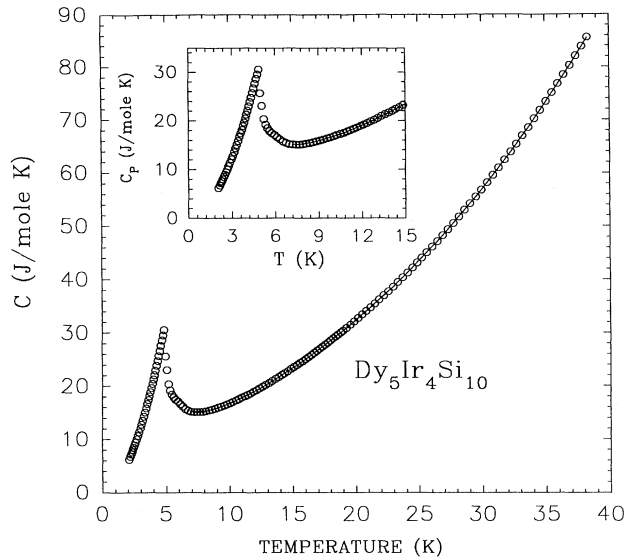


FIG. 2. The temperature dependence of the heat capacity of $\text{Dy}_5\text{Ir}_4\text{Si}_{10}$ from 2 to 36 K. The inset shows the same plot at low temperature with a λ -type transition at 5 K.

As in the case of $\text{Dy}_5\text{Ir}_4\text{Si}_{10}$, a linear behavior in C_p versus T^3 is observed for $\text{Sc}_{3.5}\text{Dy}_{1.5}\text{Ir}_4\text{Si}_{10}$, in the temperature range 15–35 K with $\beta=0.51$ mJ/mol K⁴. This sample which undergoes superconducting ordering below 5 K (Ref. 1) also shows a small anomaly in C_p near 5 K as shown in the inset of Fig. 4. The magnetic heat capacity (shown in Fig. 5) exhibits a λ -type anomaly at 3.6 K, and above 7 K a Schottky-type anomaly appears with a maximum around 26 K. The Schottky anomaly for $\text{Dy}_5\text{Ir}_4\text{Si}_{10}$ has a maximum value at 32 K whereas that of $\text{Sc}_{3.5}\text{Dy}_{1.5}\text{Ir}_4\text{Si}_{10}$ has a maximum value at 26 K. The observation of such an anomaly in both compounds sug-

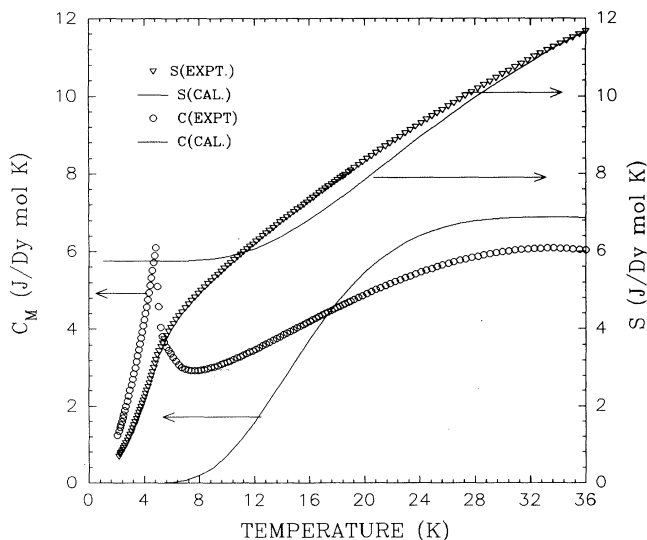


FIG. 3. The temperature dependence of the magnetic heat capacity and entropy of $\text{Dy}_5\text{Ir}_4\text{Si}_{10}$ from 2 to 36 K. A broad Schottky anomaly appears at 32 K. The solid lines are fit to the crystal-field calculations.

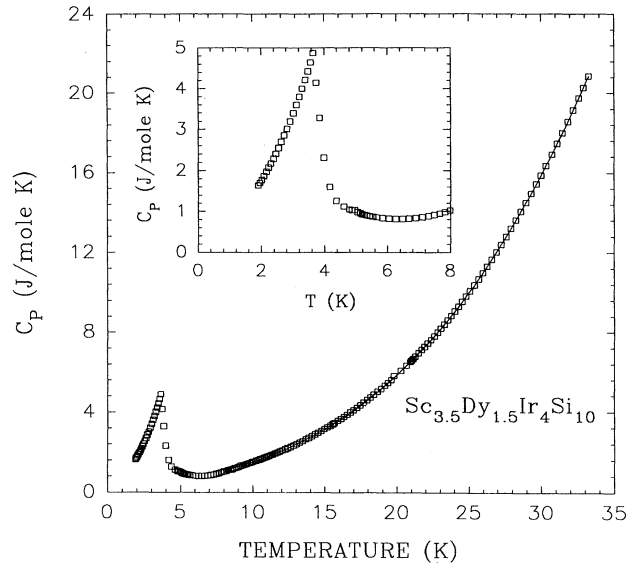


FIG. 4. The temperature dependence of the heat capacity of $\text{Sc}_{3.5}\text{Dy}_{1.5}\text{Ir}_4\text{Si}_{10}$ from 2 to 36 K. The inset shows the same plot at low temperatures with a λ -type transition at 3.5 K. One can also observe a small anomaly at 5 K which indicates the superconducting transition.

gests that the effects of the crystalline electric fields are similar in nature.

B. Crystal field analysis

The strong influence of the exchange interaction is clearly observed from low-temperature heat-capacity and magnetic-susceptibility studies. The Schottky anomaly in the magnetic heat capacity shows that there is a consider-

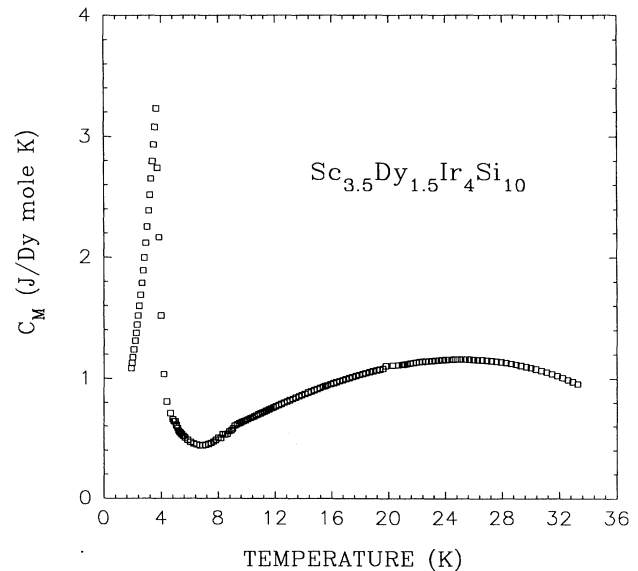


FIG. 5. The temperature dependence of the magnetic heat capacity of $\text{Sc}_{3.5}\text{Dy}_{1.5}\text{Ir}_4\text{Si}_{10}$ (obtained after the subtraction of the lattice part) from 2 to 36 K. A broad Schottky anomaly appears at 26 K.

able effect of the crystalline electric field. We have analyzed the experimental results by taking into account both crystalline electric field and exchange interactions.

The Hamiltonian of the system consisting of the spin-orbit coupling, crystalline electric field, Zeeman, and exchange field terms,

$$\mathcal{H} = \lambda \mathbf{L} \cdot \mathbf{S} + \mathcal{H}_c + \beta \mathbf{H} \cdot (\mathbf{L} + 2\mathbf{S}) + \mathcal{H}_{ex}, \quad (7)$$

is diagonalized within the substates arising from the lowest multiplet of Dy^{3+} ($J = \frac{15}{2}$) to obtain the energy and eigenfunctions of the Dy^{3+} ion. We neglected higher J multiplets to reduce the size of the matrix to be diagonalized and because they lie far off in energy¹⁴ ($> 3300 \text{ cm}^{-1}$) so that the contribution of the excited J multiplets to the susceptibility, either directly or indirectly, is negligible.

$\text{Sc}_{5-x}\text{Dy}_x\text{Ir}_4\text{Si}_{10}$ ($x = 5, 4, 1.5$) compounds crystallize in the tetragonal $\text{Sc}_5\text{Ir}_4\text{Si}_{10}$ type crystal structure and belong to the $P4/mbm$ space group. It is important to note that there are three crystallographically inequivalent sites for Sc (or Dy) in this structure, viz., Sc(1) occupies the 2(a) position, Sc(2) and Sc(3) occupy 4(h) position and all of them have different coordination (local site symmetry). At each site, because of lower symmetry, the $J = \frac{15}{2}$ state (ground multiplet) of each Dy^{3+} ion would split by the crystalline electric field to give eight different doublets. The effect of the crystalline electric field at each site would be different and the total number of crystal-field parameters representing the splitting of $J = \frac{15}{2}$ multiplets would be significantly large.

Experimentally, we observe only an average effect of the crystalline electric fields on both the magnetic susceptibility and heat capacity, which is a combined effect for all three sites. We simulate these average crystal-field effects by assuming the overall (average) crystal field to be tetragonal corresponding to the crystallographic symmetry. The Hamiltonian for such a tetragonal crystal field consists of cubic and axial distortion terms. In order to keep the number of parameters to a minimum, we retain the fourth-order cubic terms and second-order axial distortion term only. The crystal-field Hamiltonian in terms of tensor operators $C_m^{(n)}$, after retaining only these terms, can be written as¹⁵

$$\mathcal{H}_c = B_2 \sum C_0^{(2)} + B_4 \sum [C_0^{(4)} + (\frac{5}{14})^{1/2} (C_{-4}^{(4)} + C_{+4}^{(4)})]. \quad (8)$$

Thus, B_4 determines the strength of cubic crystal field while B_2 represents the strength of the axial distortion.

In the cubic crystal field, for negative B_4 , quartet ($\Gamma_8^{(1)}$) would be the ground state, whereas, for positive B_4 , doublet (Γ_6) would be the ground state. We found, that the Schottky anomaly in the observed magnetic heat capacity and the corresponding entropy could be analyzed with doublet (Γ_6) as a crystal-field ground state. We obtained a reasonably good fit to the entropy and Schottky anomaly with $B_4 = 770 \text{ cm}^{-1}$ and $B_2 = 98 \text{ cm}^{-1}$. The calculated and experimental magnetic heat capacity and entropy of $\text{Dy}_5\text{Ir}_4\text{Si}_{10}$ is shown in Fig. 3. The quality of fit to the Schottky anomaly is not very good compared to that of the magnetic-susceptibility fit (which will be described in the following section) because of the inherent error in the

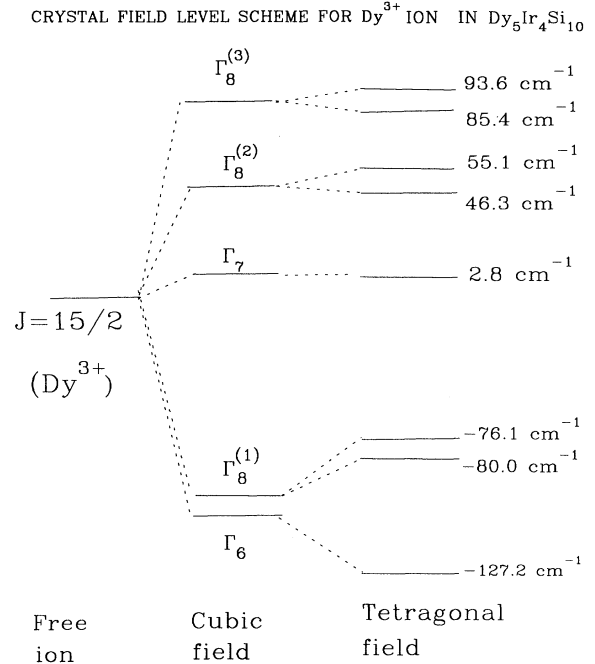


FIG. 6. A proposed crystal-field scheme for the Dy^{3+} ion in the $\text{Dy}_5\text{Ir}_4\text{Si}_{10}$ system.

subtraction of the lattice part of the heat capacity (which is also very large at these temperatures). The calculated crystalline electric-field level scheme for $\text{Dy}_5\text{Ir}_4\text{Si}_{10}$ is shown in Fig. 6.

From the Schottky anomaly data for $\text{Sc}_{3.5}\text{Dy}_{1.5}\text{Ir}_4\text{Si}_{10}$, we conclude that crystal-field effects in the $\text{Sc}_{5-x}\text{Dy}_x\text{Ir}_4\text{Si}_{10}$ ($x = 5, 4, 1.5$) series of compounds are similar with $B_4 = 770 \text{ cm}^{-1}$ and $B_2 = 98 \text{ cm}^{-1}$ as in $\text{Dy}_5\text{Ir}_4\text{Si}_{10}$. The temperature dependences of the experimental magnetic susceptibilities of $\text{Sc}_{5-x}\text{Dy}_x\text{Ir}_4\text{Si}_{10}$ in the entire range of temperature 2–300 K for $x = 5, 4$, and 1.5 are shown in Figs. 7, 8, and 9, respectively. The λ -type anomaly in the heat capacity and cusp in the magnetic susceptibility at low temperatures show that the compounds $\text{Sc}_{5-x}\text{Dy}_x\text{Ir}_4\text{Si}_{10}$ for $x = 5, 4$, and 1.5 order antiferromagnetically below 5.0, 4.5, and 3.6 K, respectively. The sharp drop in χ below 7 K for the $x = 1.5$ sample is due to the onset of superconductivity in this sample at 5 K.

The exchange interaction, in the molecular field framework, above the Néel temperature is given by

$$\mathcal{H}_{ex} = -2zJ \langle \mathbf{S} \rangle \cdot \mathbf{S}. \quad (9)$$

Here z is the number of nearest equivalent neighbors interacting with the exchange interaction J , and $\langle \mathbf{S} \rangle$ is the expectation value of the spin operator \mathbf{S} . An iterative procedure is used to calculate $\langle \mathbf{S} \rangle$ self-consistently. The details of this procedure are discussed by Marathe and Mitra.¹⁶ In our analysis, zJ would represent the average exchange interaction for all the three sites with their respective neighbors.

We have fixed the crystal-field parameters, B_4 and B_2 , obtained from the analysis of the heat-capacity data of

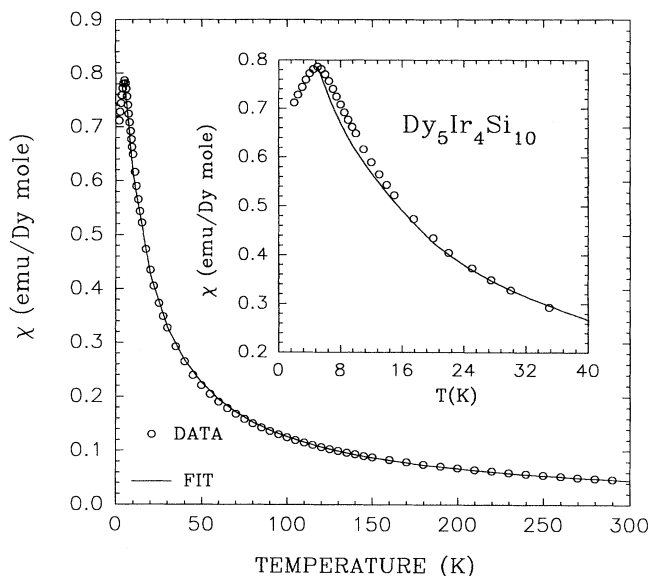


FIG. 7. The temperature dependence of the susceptibility of $\text{Dy}_5\text{Ir}_4\text{Si}_{10}$ from 2 to 300 K. The inset shows the same plot at low temperatures with an antiferromagnetic transition at 5 K. The solid line is a fit from the crystal-field model.

the compound $\text{Dy}_5\text{Ir}_4\text{Si}_{10}$ and varied the exchange parameter zJ to get the best fit to the experimentally observed magnetic-susceptibility data of $\text{Sc}_{5-x}\text{Dy}_x\text{Ir}_4\text{Si}_{10}$ ($x=5,4,1.5$) compounds. The calculated magnetic susceptibility agrees very well with the experimentally observed data of $\text{Sc}_{5-x}\text{Dy}_x\text{Ir}_4\text{Si}_{10}$ ($x=5,4,1.5$) in the entire temperature range of 5–300 K for $zJ=-1.10$, -0.83 , and -0.93 cm^{-1} , respectively. The calculated and experimentally observed susceptibilities are shown in the Figs. 7–9. Note that the ratio of zJ for $x=4$ and 5 (0.8) matches approximately with the respective ratio of T_N

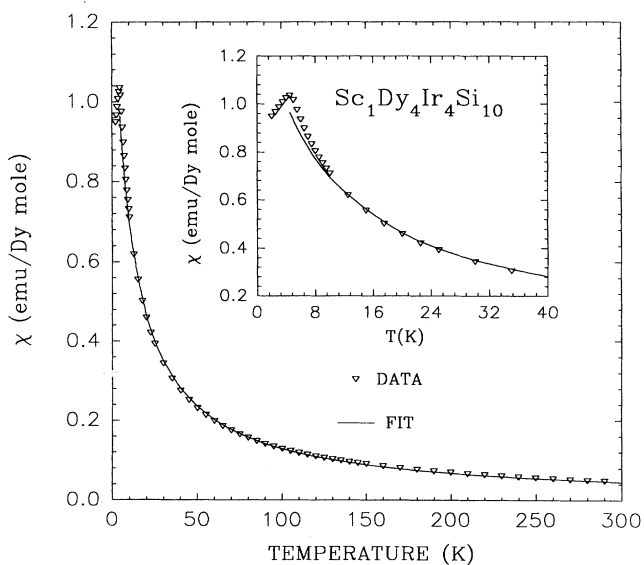


FIG. 8. The temperature dependence of the susceptibility of $\text{Sc}_1\text{Dy}_4\text{Ir}_4\text{Si}_{10}$ from 2 to 300 K. The inset shows the same plot at low temperatures with an antiferromagnetic transition at 4.5 K. The solid line is a fit from the crystal-field model.

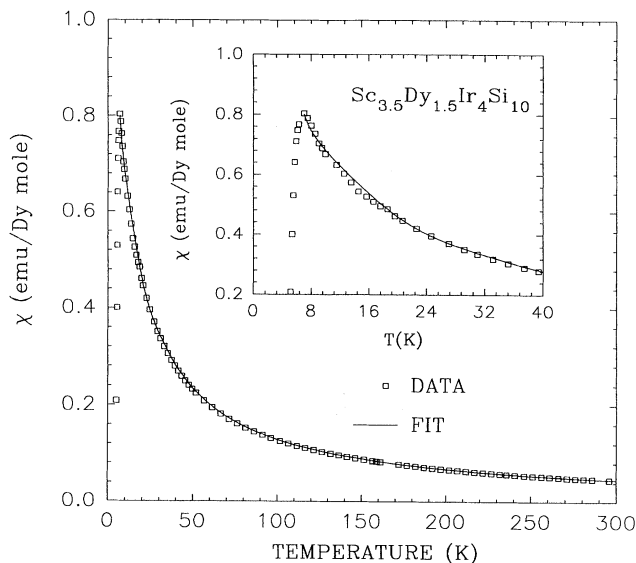


FIG. 9. The temperature dependence of the susceptibility of $\text{Sc}_{3.5}\text{Dy}_{1.5}\text{Ir}_4\text{Si}_{10}$ from 2 to 300 K. The inset shows the same plot at low temperatures with an antiferromagnetic transition at 3.5 K. The solid line is a fit from the crystal-field model.

(0.9). The large value of zJ for $\text{Sc}_{3.5}\text{Dy}_{1.5}\text{Ir}_4\text{Si}_{10}$ is unrealistic because of the coexistence of superconductivity and magnetism at low temperatures. The magnetic susceptibility of $\text{Dy}_{1.5}\text{Sc}_{3.5}\text{Ir}_4\text{Si}_{10}$ shows that the effect of superconductivity starts setting up at temperatures much higher than 7 K, at which it becomes a superconductor. Therefore, near the superconducting transition temperature, the paramagnetic susceptibility gets significantly reduced; thus, the increase in the value of the parameter zJ .

C. Coexistence of magnetism and superconductivity

In general, introduction of magnetic atoms in a superconductor decreases its transition temperature due to strong pair breaking. This pair breaking arises because of the exchange interaction of the conduction electrons with the localized magnetic moment. However, in the case of chalcogenides and rhodium borides,¹ the exchange interaction between the conduction electrons and the localized magnetic moments is small and it is of the order $I \approx 0.01 \text{ eV}$.¹ The small magnitude of I enables both RRh_4B_4 and RMO_6S_8 compounds to retain their superconductivity even in the presence of a relatively large concentration of rare-earth magnetic moments, which results in magnetic ordering via indirect Ruderman-Kittel-Kasuya-Yosida interaction at low temperatures that are comparable to superconducting transition temperatures. The reason for the small magnitude of the exchange interaction lies in the structure of these compounds. For instance, in the case of RMO_6S_8 ,¹⁷ the rare-earth atom occupies the first site at the rhombohedral cell and therefore they are situated far away from Mo atoms, which results in weak d - f exchange.

In the case of the $\text{R}_5\text{Ir}_4\text{Si}_{10}$ system, there are no transition-metal clusters and this structure can be described by the stacking of the two types of building blocks, trigonal prisms SiSc_6 and distorted tetragonal an-

tipisms IrSi_4Sc_4 .⁵ All Ir-Si and Si-Si distances are short (2–2.5 Å), which indicates strong covalent interactions. As we have mentioned earlier, the Sc atoms have three different sites to occupy and the substituted Dy atom can occupy any one of these sites. The bond distance between Sc in one of the three sites with Ir atoms is of the order of 3 Å, whereas the minimum distance between any two Sc sites is greater than 5 Å. These distances are probably large enough so that the exchange interaction between the magnetic moment of Dy and the conduction electrons is weak. The weak depression of T_c with x in $\text{Sc}_{5-x}\text{Dy}_x\text{Ir}_4\text{Si}_{10}$ (Refs. 2 and 3) supports this view. In chalcogenides and borides, one observes an anomaly in the H_{c2} vs T curve near T_N in samples which show coexistence of antiferromagnetic ordering and superconductivity.^{18,19} This has been attributed to various factors such as the reduction in electron-electron interaction by antiferromagnetic magnons, the increase in pair breaking due to moment fluctuations near T_N , etc.²⁰ Our preliminary study on the H_{c2} of $\text{Sc}_{3.5}\text{Dy}_{1.5}\text{Ir}_4\text{Si}_{10}$ (Ref. 12) shows no such anomaly near T_N . This suggests that the influence of antiferromagnetic ordering on superconductivity is very small in these compounds.

IV. CONCLUSION

We have established the bulk antiferromagnetic ordering in $\text{Dy}_5\text{Ir}_4\text{Si}_{10}$ at 5 K and the coexistence of superconductivity and magnetism in $\text{Sc}_{3.5}\text{Dy}_{1.5}\text{Ir}_4\text{Si}_{10}$. The Dy samples show a Schottky anomaly in the magnetic heat at 32 K and 26 K for $x=5.0$ and $x=1.5$. This anomaly arises due to crystal-field effects of the Dy^{3+} ion. Since Dy has three sites in $\text{Dy}_5\text{Ir}_4\text{Si}_{10}$, we assumed the overall crystal field (average) to be tetragonal and considered a crystal-field Hamiltonian up to fourth-order cubic and second-order axial terms. This simple analysis (with exchange interaction) gave consistent results for a crystal-field scheme for the Dy ion which could be fitted to both χ as well as C_p data. However, the final confirmation of this model requires detailed neutron-scattering measurements on this system.

ACKNOWLEDGMENT

We would like to thank K. V. Gopalakrishnan for performing the magnetic susceptibility measurements.

*On leave of absence from Uppsala University, Uppsala, Sweden.

¹Superconductivity in Ternary Compounds, edited by M. B. Maple and Ø. Fisher (Springer-Verlag, Berlin, 1984), Vol. II.

²H. F. Braun and M. Pelizzone, in *Superconductivity in d- and f-band metals*, edited by W. Buckel and W. Weber (KEK, Karlsruhe, 1982), p. 245–248.

³S. Ramakrishnan, K. Ghosh, and Girish Chandra, Phys. Rev. B **46**, 2952 (1992).

⁴K. Ghosh, S. Ramakrishnan, and Girish Chandra, Phys. Rev. B **48**, 10 440 (1993).

⁵K. Ghosh, S. Ramakrishnan, and Girish Chandra, Phys. Rev. B **45**, 10 769 (1992).

⁶H. F. Braun *et al.*, Acta Crystallogr. Sec. B **36**, 2397 (1980).

⁷S. Ramakrishnan, S. Sundaram, R. S. Pandit, and Girish Chandra, J. Phys. E **18**, 650 (1985).

⁸L. S. Hausermann-Berg and R. N. Shelton, Phys. Rev. B **35**, 6659 (1987).

⁹L. S. Hausermann-Berg and R. N. Shelton, Physica B+C **135B**, 400 (1985).

¹⁰G. R. Stewart, G. P. Meisner, and H. C. Ku, in *Proceedings of the IV International Conference in d- and f-band superconduc-*

tivity, edited by W. Buckel and W. Weber (Kernforschungszentrum, Karlsruhe, 1982), p. 81.

¹¹W. L. McMillan, Phys. Rev. **167**, 331 (1967).

¹²K. Ghosh, S. Ramakrishnan, A. K. Nigam, and Girish Chandra, J. Appl. Phys. **73**, 6637 (1993).

¹³T. P. Orlando, E. J. McNiff, Jr., S. Foner, and M. R. Beasley, Phys. Rev. B **19**, 4545 (1979).

¹⁴G. H. Dieke, *Spectra and Energy Levels of Rare Earth Ions in Crystals* (Interscience, New York, 1968).

¹⁵B. G. Wybourne, *Spectroscopic Properties of Rare Earths* (Interscience, New York, 1965).

¹⁶V. R. Marathe and S. Mitra, J. Chem. Phys. **78**, 915 (1983).

¹⁷Ø. Fisher, Appl. Phys. **16**, 1 (1978).

¹⁸W. Thomlinson, G. Shirane, D. E. Moncton, Y. Ishikawa, and Ø. Fisher, Phys. Rev. B **23**, 4455 (1981).

¹⁹H. C. Hamaker, L. D. Woolf, H. B. MacKay, Z. Fisk, and M. B. Maple, Solid State Commun. **32**, 289 (1979).

²⁰M. Ishikawa, Ø. Fisher, and J. Muller, in *Superconductivity in Ternary Compounds II*, edited by M. B. Maple and Ø. Fisher, Topics in Current Physics Vol. 34 (Springer-Verlag, Berlin, 1982), p. 143.